# ON REFORMULATING THE ERM-BASED SECOND-MOMENT CLOSURE TOWARDS A MORE ROBUST TURBULENCE MODEL

**J. Hui and S. Obi**
Department of Mechanical Engineering, Keio University
Hiyoshi 3-14-1, Yokohama, Japan
huijing@z6.keio.jp, obsn@mech.keio.ac.jp

**S. Jakirlić**
Institute of Fluid Mechanics and Aerodynamics / Center of Smart Interfaces, Technische Universität Darmstadt
Petersenstr. 30 / 32, D-64287 Darmstadt, Germany
s.jakirlic@sla.tu-darmstadt.de

## ABSTRACT

The present study considers a reformulation of the Durbin's (1993) ERM-based second-moment closure model aiming at reduction of the numerical stiffness originating from the wall boundary conditions. The reformulation performed represents an analogy to the procedure Hanjalic et al. (2004) proposed when deriving the eddy-viscosity-based $\zeta - f$ model. The presently reformulated model alternatively solves the transport equations for the ratio of the Reynolds stress components to turbulent kinetic energy $\zeta_{ij} = \overline{u_i u_j}/k$, instead of equations governing the Reynolds stress tensor. It is believed that the boundary conditions of the newly derived elliptic relaxation equations will contribute to the numerical robustness of the model with respect to the immediate wall vicinity. Another advantage, analogously to the Hanjalic's et al. $\zeta - f$ model, is the appearance of the Reynolds stress production rate (representing an exact formulation) in the $\zeta_{ij}$ equations instead of dissipation rate $\varepsilon$ (originating from the corresponding model equation). Application of the present model formulation to a plane channel flow in a range of Reynolds numbers up to $Re_\tau = 2003$ results in a good agreement with available DNS database.

## Introduction

The application of the elliptic relaxation method (ERM), introduced by Durbin (1993), led to a substantial improvement of the modelling of the velocity-pressure gradient correlation in the second-moment closure models. This method has a solid theoretical basis whose application avoids the use of empirical wall-damping functions. However, the implementation of the method suffers numerical difficulties due to boundary conditions in the elliptic relaxation equations, which make the computations sensitive to the near-wall grid resolution. Contrary to the majority of other near-wall turbulence models, this method does not tolerate very small $y^+$-values at the wall-closest grid nodes. The same numerical problems also appear in the ERM-based eddy viscosity model (EVM) version, denoted by $\overline{v^2} - f$ model, proposed by Durbin in 1991. In order to reduce the problem of the numerical stiffness Hanjalić et al. (2004) proposed solving the transport equation for the velocity scales ratio $\zeta = \overline{v^2}/k$ ($\propto y^2$) instead of $\overline{v^2}$ ($\propto y^4$) to make the model more robust. Similar model version has also been formulated by Laurence et al. (2004). No such efforts have been done for the ERM-based second-moment closure models. It should be furthermore recalled that the ERM-based integration is concentrated only to the near-wall region contributing strongly to the correct damping of the eddy-viscosity by approaching the solid wall. However, in the off-wall region the EVM models reduce to their high-Reynolds number counterpart, representing the standard $k - \varepsilon$ model of turbulence, being burdened by all known weaknesses: the production rate of $k$ (representing an exact term in second-moment closures) is modeled (no sensitivity to the sign change of the mean velocity gradients), the model performs purely in the transitional flows and flows affected by swirl and rotation. In the complex turbulent and transitional flows the prediction of the complete stress field may be important. The second-moment closure models are inherently capable of capturing all essential mean flow and turbulence features. Here, we proposed an ERM-version of the second-moment closure model group. Similar to the strategy taken by Hanjalić et al. (2004), we solve the transport equations for the variable $\zeta_{ij} = \overline{u_i u_j}/k$, instead of equations for $\overline{u_i u_j}$. The linear LRR-IP model (Launder et al., 1975) and its version comprising the quadratic formulation of the slow pressure-strain term (Jakirlić and Jester-Zürker, 2010) are applied as the homogeneous pressure-strain term ($\phi_{ij}^h$) models in the $f_{ij}$ equations. The predictive performance of this new model formulation is tested in a channel flow configuration at different flow Reynolds numbers.

## Model of Durbin

In the ERM-based full Reynolds stress model of Durbin (1993) the elliptic relaxation equation for the function $f_{ij} = \Pi_{ij}/k$ reads:

$$L^2 \nabla^2 f_{ij} - f_{ij} = -\frac{1}{k}\phi_{ij}^h \qquad (1)$$

$L$ is the length scale and $\phi_{ij}^h$ is the homogeneous part of the pressure-strain correlation for which any high Reynolds number model may be adopted. The length scale $L$ is defined as:

$$L = C_L \max\left[\frac{k^{2/3}}{\varepsilon}, C_\eta\left(\frac{\nu^3}{\varepsilon}\right)^{1/4}\right] \tag{2}$$

where $\varepsilon$ is the dissipation rate of $k$ and $\nu$ is the kinematic viscosity coefficient. The model constants $C_L$ and $C_\eta$ are fixed to 0.2 and 80.0, respectively.

The equation governing the Reynolds stress tensor is:

$$\frac{D\overline{u_iu_j}}{Dt} = P_{ij} + kf_{ij} + \mathscr{D}_{ij}^{\nu} + \mathscr{D}_{ij}^{t} - \frac{\overline{u_iu_j}}{k}\varepsilon \tag{3}$$

where $P_{ij}$ ,$\mathscr{D}_{ij}^{\nu}$ and $\mathscr{D}_{ij}^{t}$ stand for production, molecular diffusion and turbulent diffusion. The model by Daly and Harlow (1970) is adopted for the turbulent diffusion in an appropriately modified form:

$$\mathscr{D}_{ij}^{t} = -\frac{\partial}{\partial x_l}\left(\frac{c_\mu}{\sigma_k}T\overline{u_lu_m}\frac{\partial\overline{u_iu_j}}{\partial x_m}\right) \tag{4}$$

with $c_\mu = 0.23$ and $\sigma_k = 1.0$. The time scale $T$ is defined as:

$$T = \max\left[\frac{k}{\varepsilon}, C_T\left(\frac{\nu}{\varepsilon}\right)^{1/2}\right] \tag{5}$$

where $C_T = 6.0$.

Velocity-pressure gradient correlation $\Pi_{ij}$ is modeled jointly with the stress dissipation tensor $\varepsilon_{ij}$:

$$kf_{ij} = \Pi_{ij} - \varepsilon_{ij} + \frac{\overline{u_iu_j}}{k}\varepsilon \tag{6}$$

Eq. (1) then becomes:

$$L^2\nabla^2 f_{ij} - f_{ij} = -\frac{1}{k}\left(\phi_{ij}^h + a_{ij}\varepsilon\right) \tag{7}$$

with $a_{ij} = \overline{u_iu_j}/k - (2/3)\delta_{ij}$. In the homogeneous limit, it is assumed that $\varepsilon_{ij} = (2/3)\varepsilon\delta_{ij}$.

For statistically two-dimensional flows, one shear stress component, $\overline{uv}$, and two normal stress components, $\overline{u^2}$ and $\overline{v^2}$, are to be calculated, and the remaining normal stress component, $\overline{w^2}$, is subsequently determined from the relation $\overline{w^2} = 2k - \overline{u^2} - \overline{v^2}$. The boundary conditions for $f_{ij}$ are:

$$f_{11} = 0,\ \ f_{22} = -\frac{20\nu^2}{\varepsilon}\frac{\overline{v^2}}{y_1^4},\ \ f_{12} = -\frac{20\nu^2}{\varepsilon}\frac{\overline{uv}}{y_1^4} \tag{8}$$

with $y_1$ representing the distance from the wall to the next grid node. They are derived based on the examination of the budgets of the Reynolds stress transport equations in the near-wall region. The boundary conditions cause numerical problems because the rapid change of the Reynolds stresses appearing in the numerator is magnified by the small denominator value being proportional to $y_1^4$ (Eq. 8).

## Present formulation

In the present study, the transport equations of $\zeta_{ij} \equiv \overline{u_iu_j}/k$ are solved instead of equations of Reynolds stresses $\overline{u_iu_j}$. Following the definition of $\zeta_{ij}$, the transport equations of $\zeta_{ij}$ are derived from the equations of $\overline{u_iu_j}$ and $k$:

$$\begin{aligned}\frac{D\zeta_{ij}}{Dt} &= \frac{P_{ij}}{k} + f_{ij} - \frac{P_k}{k}\zeta_{ij} + \nu\nabla^2\zeta_{ij} \\ &+ \frac{\partial}{\partial x_l}\left(\frac{c_\mu}{\sigma_k}k\zeta_{lm}T\frac{\partial\zeta_{ij}}{\partial x_m}\right) + 2\frac{\nu}{k}\frac{\partial\zeta_{ij}}{\partial x_k}\frac{\partial k}{\partial x_k} \\ &+ \frac{2}{k}\left(\frac{c_\mu}{\sigma_k}k\zeta_{lm}T\right)\frac{\partial\zeta_{ij}}{\partial x_l}\frac{\partial k}{\partial x_m}\end{aligned} \tag{9}$$

with $P_{ij} = -k\zeta_{ik}\partial\overline{U_j}/\partial x_k - k\zeta_{jk}\partial\overline{U_i}/\partial x_k$ and $P_k = (1/2)P_{ii}$.

The last two cross-derivative terms arose as a consequence of the transformation of transport equation for $\overline{u_iu_j}$ into $\zeta_{ij}$-equation. Hanjalić et al. (2004) omitted such terms for simplicity. The compensation was made by re-tuning some of the model coefficients. Here, we kept the both cross-derivative terms because the check of the budgets of the $\zeta_{ij}$ equations in a channel flow indicated that they can not be neglected (see corresponding discussion later). As the consequence of this transformation the stress dissipation tensor $\varepsilon_{ij}$ does not appear in the transport equations of $\zeta_{ij}$. The production rate $P_k$ appears instead, which represents an advantage because the $\varepsilon_{ij}$-components are difficult to be correctly reproduced in the near-wall region, while $P_k$ is an exact term and needs no modeling.

For the homogeneous pressure-strain model term, we adopted both the LRR-IP model (Launder et al., 1975):

$$\Phi_{ij}^h = -c_1\varepsilon_{ij} - c_2\left(P_{ij} - \frac{2}{3}P_k\delta_{ij}\right) \tag{10}$$

with $c_1 = 1.22$, $c_2 = 0.6$, and the LRR-IP model extended to account for the non-linearity in the slow pressure-strain term (Jakirlić and Jester-Zürker, 2010):

$$\Phi_{ij}^h = -c_1\varepsilon_{ij} - c_1^{'}\varepsilon(a_{ik}a_{jk} - \frac{1}{3}\delta_{ij}A_2) - c_2\left(P_{ij} - \frac{2}{3}P_k\delta_{ij}\right) \tag{11}$$

with $A_2 = a_{ij}a_{ji}$, $a_{ij} = \zeta_{ij} - 2/3\delta_{ij}$, $c_1 = 1.5$, $c_1^{'} = \max[0.7A_2; 0.5]c_1$ and $c_2 = 0.6$.

The transport equations for $k$ and $\varepsilon$ are:

$$\frac{Dk}{Dt} = -k\zeta_{lm}\frac{\partial\overline{U_l}}{\partial x_m} - \varepsilon + \nu\nabla^2 k + \frac{\partial}{\partial x_l}\left(\frac{c_\mu}{\sigma_k}k\zeta_{lm}T\frac{\partial k}{\partial x_m}\right) \tag{12}$$

$$\frac{D\varepsilon}{Dt} = -c_{\varepsilon 1}^{'}\frac{k}{T}\zeta_{lm}\frac{\partial\overline{U_l}}{\partial x_m} - c_{\varepsilon_2}\frac{\varepsilon}{T} + \frac{\partial}{\partial x_l}\left(\nu\delta_{lm} + \frac{c_\mu}{\sigma_\varepsilon}k\zeta_{lm}T\frac{\partial\varepsilon}{\partial x_m}\right) \tag{13}$$

with $c_{\varepsilon 1}^{'} = -c_{\varepsilon 1}(1 + a_1P_k/\varepsilon)$, $c_{\varepsilon 1} = 1.44$, $a_1 = 0.1$, $c_{\varepsilon 2} = 1.9$ and $\sigma_\varepsilon = 1.65$.

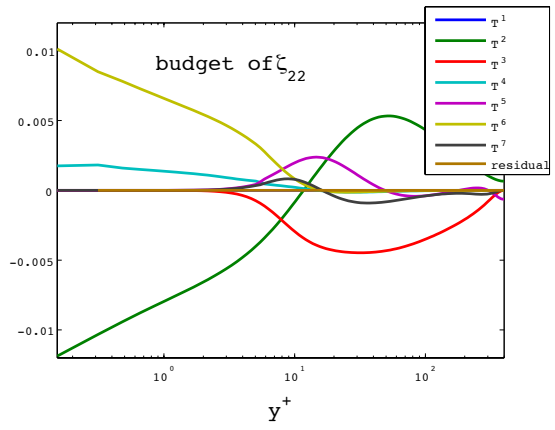


(a)

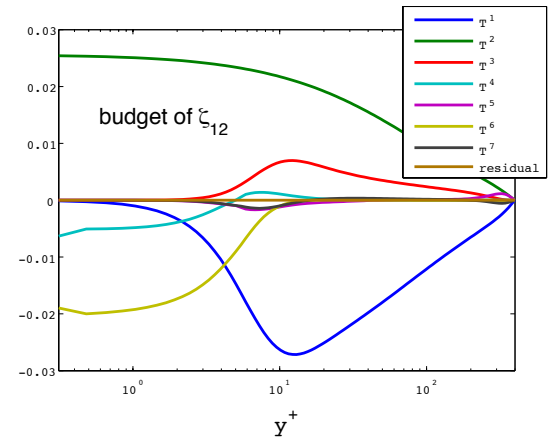


(b)

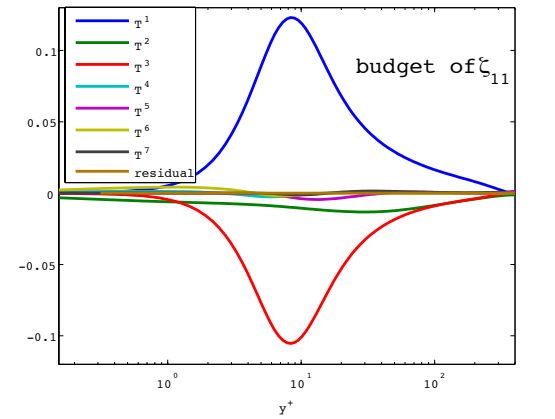


(c)

Figure 1. Budgets of the $\zeta_{ij}$-equation: (a) $\zeta_{22}$, (b) $\zeta_{12}$, (c) $\zeta_{11}$. $T^1$: $P_{ij}/k$; $T^2$: $f_{ij}$; $T^3$: $-P_k/k\zeta_{ij}$; $T^4$: $\nu d^2\zeta_{ij}/dy^2$; $T^5$: $d(c_\mu/\sigma_k k\zeta_{22}T)d\zeta_{ij}/dy$; $T^6$: $2\nu/kd\zeta_{ij}/dydk/dy$; $T^7$: $2/k(c_\mu/\sigma_k k\zeta_{22}T)d\zeta_{ij}/dydk/dy$.

## Boundary conditions

Provided that the fluctuating velocity can be expanded in terms of the wall distance $y$:

$$u_i = a_i + b_i y + c_i y^2 + \dots \tag{14}$$

the wall values of $\zeta_{ij}$ can be derived as:

$$\zeta_{22} = \zeta_{12} = 0 \tag{15}$$

and

$$\zeta_{11} = \frac{2\overline{b_1 b_1}}{\overline{b_1 b_1} + \overline{b_3 b_3}} \tag{16}$$

The boundary condition of $\zeta_{11}$ indicates its finite value at the wall, though it is not known. For the fully developed channel flows it is found that $\zeta_{11}$ has a fairly weak dependence on the Reynolds numbers. Therefore, in our practical applications, we use a finite value originating from the DNS database (only) at the start of the iteration procedure, while the boundary condition is specified as:

$$\left.\frac{\partial \zeta_{11}}{\partial y}\right|_{wall} = 0 \tag{17}$$

which is quite reasonable and we met no practical difficulties.

The balance between leading terms in the $\zeta_{ij}$-equation becomes in the near-wall region:

$$\lim_{y\to 0}\left(f_{ij} + \nu\nabla^2\zeta_{ij} + 2\frac{\nu}{k}\frac{\partial\zeta_{ij}}{\partial x_k}\frac{\partial k}{\partial x_k}\right) = 0 \tag{18}$$

from which the boundary conditions are deduced as:

$$f_{11} = 0, \quad f_{22} = \frac{-10\nu\zeta_{22}}{y_1^2}, \quad f_{12} = \frac{-4\nu\zeta_{12}}{y_1^2} \tag{19}$$

It can be seen that the denominators in the expressions for $f_{22}$ and $f_{12}$ are proportional to $y_1^2$ instead of $y_1^4$ as it was in the Durbin's ERM-based Reynolds stress model. This is an advantage with respect to the reduction of the numerical stiffness of the ERM-based models. The boundary conditions for $k$ and $\varepsilon$ are:

$$k = 0, \quad \varepsilon = \frac{2\nu k_1}{y_1^2} \tag{20}$$

with $k_1$ representing the value of $k$ at the wall-adjacent grid node.

## Formulas for the fully developed channel flow

The present model was applied to a fully developed plane channel flow. The corresponding partial differential equations were simplified to a set of the one-dimensional ordinary differential equations as follows:

• the momentum equation:

$$0 = -\frac{1}{\rho}\frac{d\overline{P}}{dx} - \frac{d\overline{uv}}{dy} + \nu\frac{d^2\overline{U}}{dy^2} \tag{21}$$

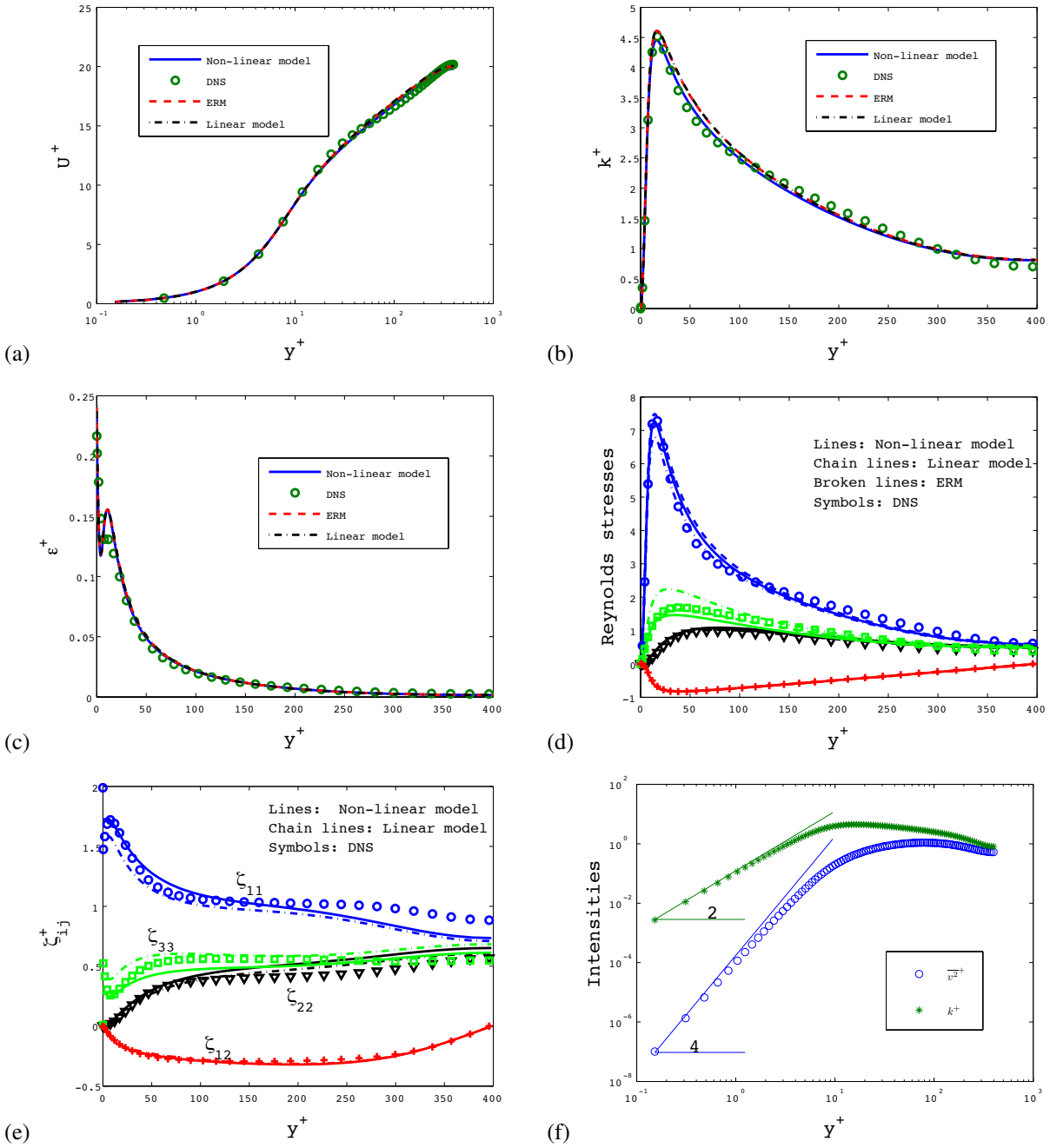


Figure 2. Results obtained by present formulations with linear and non-linear $\phi_{ij}^h$ models compared with the original ERM-model and DNS in a plane channel flow at $Re_\tau = 395$: (a) $U^+$, (b) $k^+$, (c) $\varepsilon^+$, (d) $\overline{u_i u_j}^+$, (e) $\zeta_{ij}$ and (f) asymptotic behavior of $\overline{v^2}^+$ and $k^+$ by approaching the wall.

• the transport equations for the $\zeta_{ij}$-components:

$$
\begin{aligned}
0 = & \frac{P_{11}}{k} + f_{11} - \frac{P_k}{k}\zeta_{11} + \nu\frac{d^2\zeta_{11}}{dy^2} \\
& + \frac{d}{dy}\left(\frac{c_\mu}{\sigma_k} k\zeta_{22} T \frac{d\zeta_{11}}{dy}\right) + 2\frac{\nu}{k}\frac{d\zeta_{11}}{dy}\frac{dk}{dy} \\
& + \frac{2}{k}\left(\frac{c_\mu}{\sigma_k} k\zeta_{22} T\right)\frac{d\zeta_{11}}{dy}\frac{dk}{dy}
\end{aligned}
\tag{22}
$$

$$
\begin{aligned}
0 = & f_{22} - \frac{P_k}{k}\zeta_{22} + \nu\frac{d^2\zeta_{22}}{dy^2} \\
& + \frac{d}{dy}\left(\frac{c_\mu}{\sigma_k} k\zeta_{22} T \frac{d\zeta_{22}}{dy}\right) + 2\frac{\nu}{k}\frac{d\zeta_{22}}{dy}\frac{dk}{dy} \\
& + \frac{2}{k}\left(\frac{c_\mu}{\sigma_k} k\zeta_{22} T\right)\frac{d\zeta_{22}}{dy}\frac{dk}{dy}
\end{aligned}
\tag{23}
$$

$$0 = \frac{P_{12}}{k} + f_{12} - \frac{P_k}{k}\zeta_{12} + \nu\frac{d^2\zeta_{12}}{dy^2} + \frac{d}{dy}\left(\frac{c_\mu}{\sigma_k}k\zeta_{22}T\frac{d\zeta_{12}}{dy}\right) + 2\frac{\nu}{k}\frac{d\zeta_{12}}{dy}\frac{dk}{dy} + \frac{2}{k}\left(\frac{c_\mu}{\sigma_k}k\zeta_{22}T\right)\frac{d\zeta_{12}}{dy}\frac{dk}{dy} \quad (24)$$

• the elliptic relaxation equations for $f_{ij}$-components:

$$L^2\frac{d^2 f_{11}}{dy^2} - f_{11} = \frac{2}{3T} - \frac{\zeta_{11}}{T} - \frac{\phi^h_{11}}{k} \quad (25)$$

$$L^2\frac{d^2 f_{22}}{dy^2} - f_{22} = \frac{2}{3T} - \frac{\zeta_{22}}{T} - \frac{\phi^h_{22}}{k} \quad (26)$$

$$L^2\frac{d^2 f_{12}}{dy^2} - f_{12} = -\frac{\zeta_{12}}{T} - \frac{\phi^h_{12}}{k} \quad (27)$$

• the transport equation for $k$:

$$0 = -k\zeta_{12}\frac{d\overline{U}}{dy} - \varepsilon + \frac{d}{dy}\left(\nu + \frac{c_\mu}{\sigma_k}\zeta_{22}T\right)\frac{dk}{dy} \quad (28)$$

• the transport equation for $\varepsilon$:

$$0 = \frac{c'_{\varepsilon 1}P_k - c_{\varepsilon 2}\varepsilon}{T} + \frac{d}{dy}\left(\nu + \frac{c_\mu}{\sigma_\varepsilon}\zeta_{22}T\right)\frac{d\varepsilon}{dy} \quad (29)$$

## Results

The equations were solved by means of finite difference method. All spatial derivatives were discretized by a second-order central differencing scheme. A non-uniform grid system of totally 201 grid points in the wall-normal direction was used. Because of the strongly coupled non-linear equations, a pseudo temporal scheme was introduced. All results are normalized by friction velocity $u_\tau$ and kinematic viscosity $\nu$.

Fig. 1 depicts the budgets of $\zeta_{ij}$-equations corresponding to the present model with the non-linear $\phi^h_{ij}$ formulation at $Re_\tau = 395$. The cross-derivative terms $2\nu/k(d\zeta_{22}/dy)(dk/dy)$ and $2\nu/k(d\zeta_{12}/dy)(dk/dy)$ being balanced by the elliptic relaxation functions $f_{22}$ and $f_{12}$ respectively display a certain influence in the near-wall region. The last cross-derivative term on the right hand side of Eq. (9) is negligible for all three components, but as it may be important in more complex flows it is retained in the present model.

Fig. 2 shows the results obtained by the present model at $Re_\tau = 395$, combined with both linear and non-linear $\phi^h_{ij}$ formulations, compared with the Durbin's ERM-RSM and the DNS data (Iwamoto et al., 2002). The mean velocity $U^+$ is predicted well by both present $\phi^h_{ij}$ model formulations,

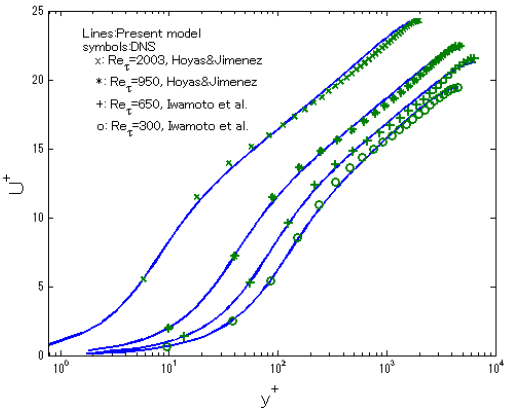


(a)

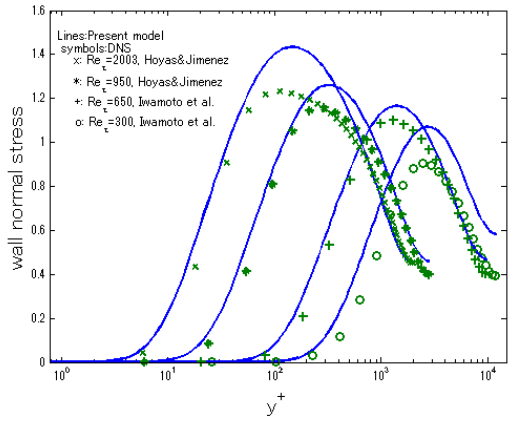


(b)

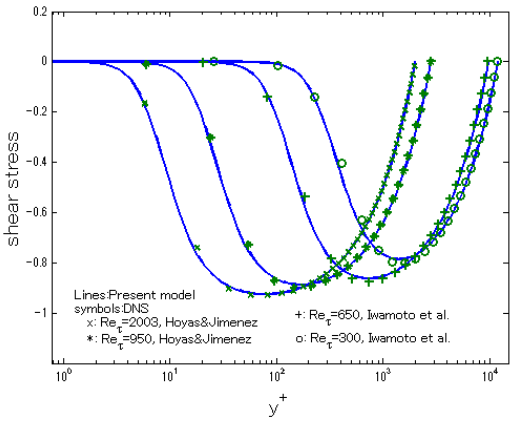


(c)

Figure 3. Channel flow at different Reynolds numbers computed by the present method with LRR-IP model: (a) $U^+$, (b) $\overline{v^2}^+$ and (c) $\overline{uv}^+$. The profiles for $Re_\tau$=300, 650 and 950 have been displaced at the $y^+$-axis for legibility.

Fig. 2(a). Turbulent kinetic energy $k^+$ exhibits somewhat better agreement by the non-linear formulation in the region $20 \le y^+ \le 100$, Fig. 2b. The predictions of the dissipation rate $\varepsilon^+$ by all three models used are of the similar quality, Fig. 2(c). Fig. 2(d) displays the Reynolds stress component pro-

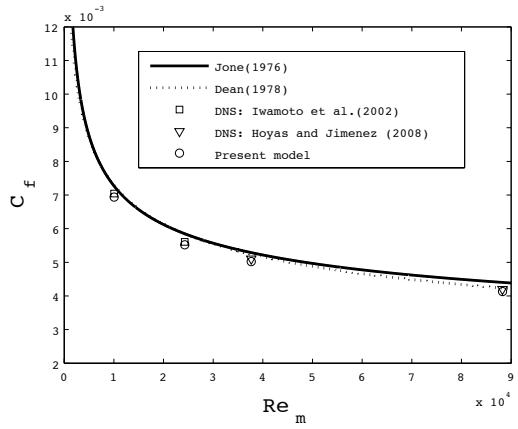


Figure 4. $C_f$ evolution in terms of $Re_m$ predicted by the present linear (LRR-IP) model formulation and compared with the DNS data and empirical solutions.

files. The $\overline{v^2}$ and $\overline{uv}$ components are predicted well by all three models. A somewhat better agreement of the $\overline{u^2}$-component is obtained in the region $20 \leq y^+ \leq 100$ when combined with the LRR-IP model. However, the peak of $\overline{u^2}$ exhibit a certain underestimation, while the $\overline{w^2}$-peak is overestimated. The adaptation of the non-linear $\phi_{ij}^h$ model version in the present formulation improves substantially the maximum values of both $\overline{u^2}$ and $\overline{w^2}$ stress components. Fig. 2(e) illustrates the prediction of the $\zeta_{ij}$ components. Some departures of $\zeta_{11}$, $\zeta_{22}$ and $\zeta_{33}$ in the area away from the wall have no noticeable effects on the prediction of the Reynolds stresses, as seen in Fig. 2(d). The asymptotic behavior of $\overline{v^2}^+$ and $k^+$ depicted in Fig. 2(f) follows closely the theoretical findings: $\overline{v^2}^+ \propto y^4$ and $k^+ \propto y^2$ (the correct asymptotic behavior of $\overline{uv} \propto y^3$ - not shown here - was also obtained). Both linear and non-linear $\phi_{ij}^h$ model formulations resulted in the same behavior, therefore only the profiles obtained by the linear model are presented.

The present model is furthermore tested at different channel flow Reynolds numbers. Fig. 3 illustrates the prediction of $U^+$, $\overline{v^2}^+$ and $\overline{uv}^+$ at different friction velocity-based Reynolds numbers $Re_\tau$ =300, 650, 950 and 2003. The results are compared with the DNS data of Iwamoto et al.(2002) at $Re_\tau = 395$ and 650 and DNS data of Hoyas and Jiménez (2008) at $Re_\tau = 950$ and 2003. Here, the present model was coupled with the linear $\phi_{ij}^+$ (actually LRR-IP) formulation. The mean velocity and the shear stress component are well reproduced across the entire channel, Fig. 4(a) and (c). The peak of the wall-normal stress component $\overline{v^2}^+$ (Fig. 3(b)) tends to be over-predicted. The employment of the non-linear model formulation (computations are in progress) should contribute to an appropriate reduction.

Fig. 4 shows the friction factor ($C_f$) development in terms of the Reynolds number ($Re_\tau = 300, 650, 950$ and 2003) predicted by the present linear model. Results are compared with the available DNS data, the Dean's:

$$C_f = 0.073 Re_m^{-0.25} \tag{30}$$

and Jones' empirical formulations:

$$\frac{1}{C_f^{0.5}} = 4log(Re_m C_f^{0.5}) \tag{31}$$

Here, $Re_m$ is the Reynolds number based on the bulk velocity $U_m$ and channel half width $\delta$. The prediction of $C_f$ is in good agreement, especially with the DNS results.

## Conclusions

The issue pertinent to numerical difficulties in the Durbin's elliptic relaxation method has been investigated in the present work. A modified formulation of the ERM-based second-moment closure model is presented, which is supposed to reduce the stiffness of the initial ERM-based model by using the equation for $\zeta_{ij} \equiv \overline{u_i u_j}$ instead of $\overline{u_i u_j}$. This yields more robust boundary conditions for the elliptic relaxation equations. Reasonable results are obtained for a plane channel flow by the proposed formulation. The performance of the modified formulation with respect to the results quality is similar to the original model. This model formulation should be further tested in more complex flow configurations.

## REFERENCES

Daly, B. J. and Harlow, F. H., 1970. "Transport equations in turbulence", Phys. Fluids,Vol.13, pp.2634-2649.

Durbin, P. A., 1991."Near-wall turbulence modeling without damping functions", Theoret. Comput. Fluid Dyn., Vol.3, pp.1-13.

Durbin, P. A., 1993. "A Reynolds stress model for near-wall turbulence", J. Fluid Mech., Vol.249, pp.465-498.

Jakirlić, S. and Jester-zürker R., 2010."Convective heat transfer in wall-bounded flows affected by severe fluid properties variations: a second-moment closure study", FEDSM-ICNMM2010.

Hanjalić, K. , Popovac, M., and Hadžiabdić, M., 2004. "A robust near-wall elliptic relaxation eddy-viscosity turbulence model for CFD", Int. J. Heat and Fluid Flow, Vol.25, pp.897-901.

Iwamoto, K., Suzuki, Y., and Kasagi, N., 2002. "Reynolds Number Effect on Wall Turbulence: Toward Effective Feedback Control", Int. J. Heat and Fluid Flow, Vol. 23, pp. 678-689.

Launder, B. E., Reece, G. J. and Rodi, W., 1975. "Progress in the development of a Reynolds-stress turbulence closure",J. Fluid Mech., Vol.68, pp.537-566.

Laurence, D. R. , Uribe, J. C., and Utyuzhnikov, S. V., 2004. "A robust formulation of the $\overline{v^2} - f$ model", Flow, turbulence and combustion, Vol.73, pp.169-185.

Hoyas S. and Jiménez J., 2008, "Reynolds number effects on the Reynolds-stress budgets in turbulent channels",Phys. Fluids, Vol.20, 101511.